

ICM11

Crack Growth Studies in Railway Axles under Corrosion Fatigue: Full-scale Experiments and Model Validation

S. Beretta^a, M. Carboni^a, A. Lo Conte^{a*}, D. Regazzi^a, S. Trasatti^b, M. Rizzi^b

^a*Politecnico di Milano, Dept. of Mechanical Engineering, Via La Masa 1, 20156 Milan, Italy*

^b*Università di Milano, Dept. of Chemistry and Electrochemistry, Via Golgi 19, 20133 Milan, Italy*

Abstract

Crack initiation and growth in full scale railway axle in A1T mild steel have been studied, under three points rotating bending loading conditions and artificial rainwater as corrosive environment. A surface plastic replication technique has been used along with optical microscopy and Scanning Electron Microscopy to monitor the environment assisted fatigue at various stages. A modified Murtaza and Akid empirical model has been employed to predict the corrosion fatigue crack growth rates and a reasonable agreement has been found between experimental and calculated lifetime.

© 2011 Published by Elsevier Ltd. Open access under [CC BY-NC-ND license](https://creativecommons.org/licenses/by-nc-nd/4.0/).
Selection and peer-review under responsibility of ICM11

"Keywords: A1T steel; Railway axles; Corrosion-fatigue; Crack Growth ;"

1. Introduction

During the railway axles' service life, fatigue is a major process resulting in structural degradation and failure. Moreover, experience with existing axles has indicated that also the corrosion is a key problem that must be addressed if maintenance costs are to be managed within acceptable limits, and if the structural reliability of the axles is to be maintained [1, 2]. Even when the axles are operated to the operating loads, failure can happen due to the synergetic effect of both corrosion and cyclic loads. This synergy is not thoroughly understood and represents an area of considerable interest to develop crack growth rate data that will allow estimates of residual strength of railway axles. In recent papers [3, 4] the authors clearly indicated that the presence of a mild aggressive environment, as the artificial rainwater, both intermittently or continuously, enhanced fatigue crack growth significantly and decrease a railway axles' lifetime drastically. In [4] the authors also analyze the pit-to-crack transition and the crack propagation mechanism in order to describe the corrosion-fatigue crack growth data with a modified Murtaza and Akid model [5].

* Corresponding author. *E-mail address:* antoinetta.loconte@polimi.it

In the present paper corrosion fatigue tests in presence of artificial rain water will be carried out on full scale axles and the predictive model for fatigue crack growth assisted by corrosion of rainwater will be applied to estimate the corrosion fatigue life of the axles.

2. Crack Growth Model

To set a suitable model for prediction of the corrosion fatigue life of railway axles, crack growth rate measurements were performed during crack propagations tests under correlate fatigue and corrosion on A1T small scale specimens [4]. Experiments at $\Delta\sigma=400$ MPa, $\Delta\sigma=320$ MPa, $\Delta\sigma=240$ MPa, have been run. The load configuration is four points rotating bending, $R=\sigma_{\min}/\sigma_{\max}=1$, under continuous dropping of aerated artificial rainwater. The composition of the artificial rainwater is Ammonium sulfate 46.2 mg/l; Sodium sulfate 31.95 mg/l; Sodium nitrate 21.25 mg/l; Sodium chloride 84.85 mg/l. During testing the PH value of the artificial rainwater is measured on daily basis and adjusted to a value between 5.7 and 6.3; the conductivity and the temperature of the artificial rainwater are monitored in order to verify that their initial values are maintained; and the free corrosion potential (E_{corr}) is plotted vs. the number of cycles. The results of the tests for each stress level are shown in the Figure 1(a)

To predict the corrosion fatigue lifetime of the A1T railway axles the Hobson-Brown model, modified in the work of Murtaza and Akid [10], is proposed. The model allows us to account for a crack growth rate dependent on the applied stress level. The corrosion fatigue crack growth rate may be described by the following equation [4]:

$$\left(\frac{da}{dN}\right) = B (\Delta\sigma)^\beta a^n \quad \rightarrow \quad \frac{da}{a^n} = B (\Delta\sigma)^\beta dN \quad (1)$$

where:

B , β , and n are the material constants (in most cases $n=1$);
 $\Delta\sigma$ is the stress range.

The results of the model for each stress level are shown in the same Figure 3(b).

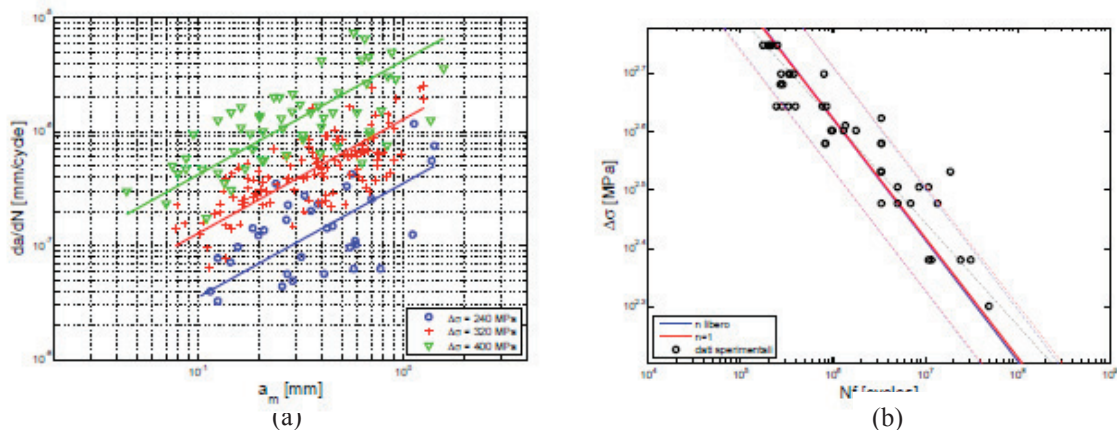


Fig. 1. (a) Corrosion fatigue on small scale specimens: crack growth experimental data and interpolation for each of the three stress level. (b) Corrosion fatigue SN diagram and description in term of corrosion fatigue crack propagation.

By adopting equation (1), we are also able to propose a description of the S-N diagram in terms of propagation of corrosion fatigue cracks from the transition length from short crack to long crack (d_m) to the final crack length (a_f). As can be seen in figure 1(b), if d_m is assumed equal to the material grain size (20 μm) and the final crack length corresponding to failure is assumed $a_f=3\text{mm}$, the prediction of the adopted model describes the median S-N diagram fairly accurately.

3. Full-scale experiments

The present study involves corrosion-fatigue tests on full scale specimens representative of common designed hollow railway axles for passenger trains in service in the Central Europe railways net. The geometry of the specimens is detailed in figure 2(a). The nominal inner and the outer diameters are the same as in axles. The press-fitting is reproduced one time in the middle of the specimens as the loading configuration, also marked in figure 2(a), is a three point bending. Smooth hour-glass shape has been designed close to the press-fitting zone for local corrosive environment application.

The material is AIT steel, widely used in the manufacture of railway axles. The matrix consists of a ferritic-pearlitic microstructure with a 20-40 μm ferritic grain size. The resultant mechanical properties are of the following order: ultimate tensile strength (UTS) 620 MPa, yield strength 390 MPa, Young's modulus 206 GPa and elongation 14.8 %.

Two full scale specimens have been tested. The experimental conditions and the corrosive environment are the same as detailed in the previous paragraph for the small scale case. The schematic of the experimental set up and a detail of the corrosion cell are visible in figure 2(b). The first test has been run at a constant amplitude test of 160 MPa, which is just below the EN13103/4 design limit ($\sigma_{\text{design}} = 166$ MPa). The second test has been run under variable amplitude loading. The load sequence is a random permutation of the scheduled stress levels. Both tests were performed at constant frequency of 8 Hz, at room temperature, and freely corroding conditions to simulate near service conditions.

Figure 3(a) shows the free corrosion potential for the test under constant amplitude loading. The initial potential is -480 mV, this is followed by a decrease in negative potential till -560 mV. At regular intervals, the dropping of the artificial rainwater has been interrupted and locally the rust layer has been removed to monitor the fatigue corrosion damage of the surface of the specimen. For this reason, a steady state of the potential has not been obtained, but jumps back to initial value are present.

The evolution of the fatigue corrosion damage, pits formation, cracks initiation and growth, has been monitored by surface replication, of small areas each 45° along the circumference at the center line of the hourglass. Corrosion causes localized pitting of the surface, and these pits serve as stress concentrations to trigger fatigue crack initiation. A high density of small cracks is observed on the surface exposed to artificial rainwater, in the early stage of the corrosion fatigue tests. Figure 3(b) shows examples of cracks initiation from corrosion pits for the test at variable amplitude, when the number of cycles is $3.2 \cdot 10^6$ cycles, about 10% of the predicted life. The synergetic action involved in the mechanics of corrosion fatigue make the threshold stress intensity factor of short cracks initiated at corner pits lower and the crack growth faster when compared to the laboratory air conditions [4]. When the number of cycles increase, the crack length increases due to the propagation of single cracks or due to the coalescence of a small number of individual cracks. The coalescence of propagating cracks results a key factor in the development of the damage and in the formation of a typical zig-zag path of the crack.

The constant amplitude test is terminated with the final failure of the specimens at $9.4 \cdot 10^6$ cycles. Magnetic particles examination of the broken specimen reveals two very long cracks, the main is about 110 mm and shows the before mentioned, zig-zag path, and a large populations of uniformly distributed cracks which length is of order of millimeters (figure 4(a)). The morphology of damage found confirmation in literature [1], where a real case of corrosion fatigue failure of railway axle is documented.

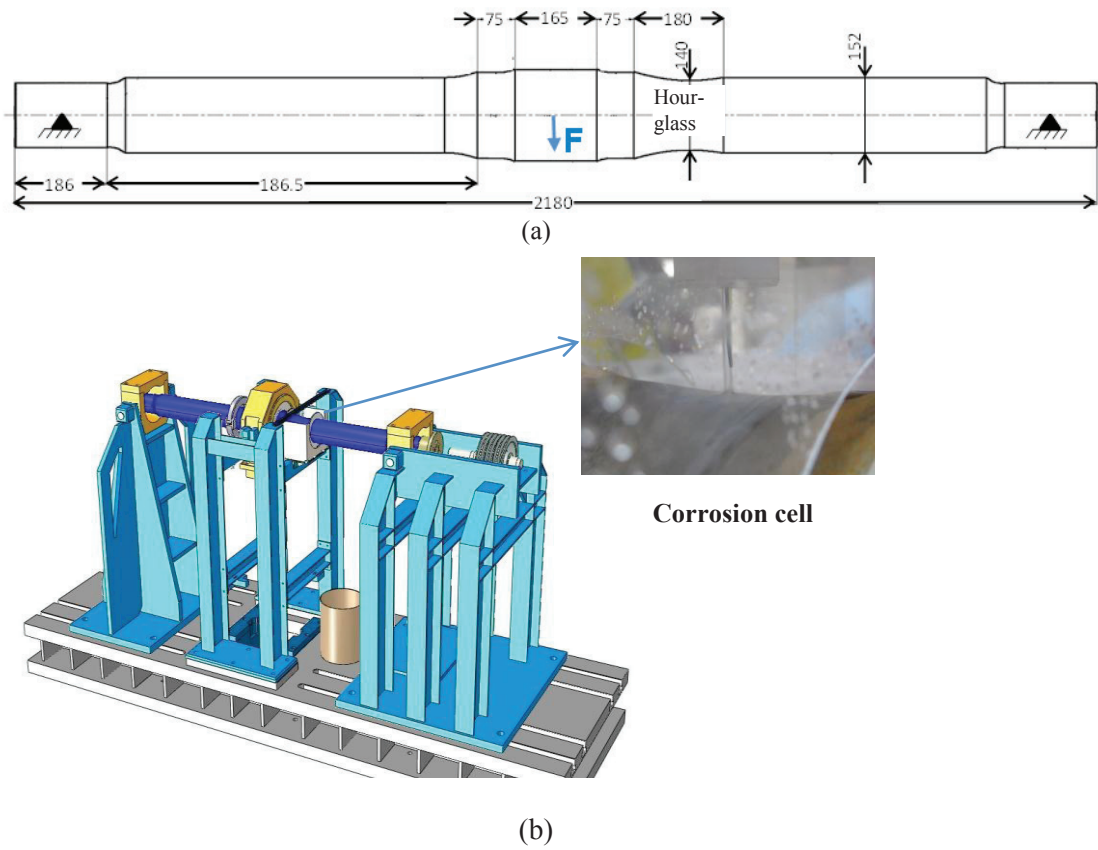


Fig. 2. (a) Full-scale specimen and load configuration; (b) Schematic of the experimental test set up for full-scale corrosion fatigue experiments and detail of the corrosion cell.

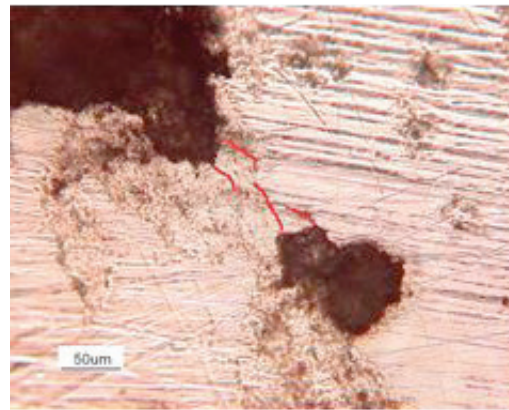
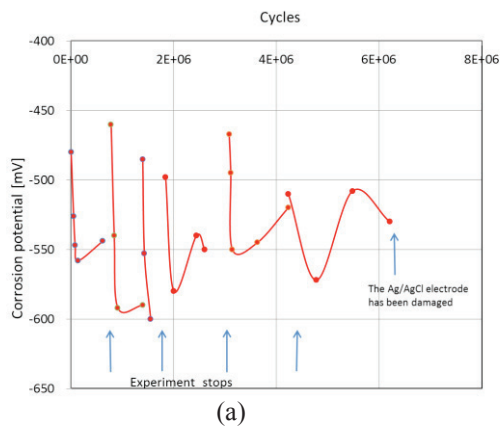


Fig. 3. (a) Free corrosion potential vs. the number of cycles for the full scale test under constant amplitude loading. (b) Cracks initiation from corrosion pits. Surface of the specimen tested at variable amplitude at $3.2 \cdot 10^6$ cycles, about 10% of the predicted life.

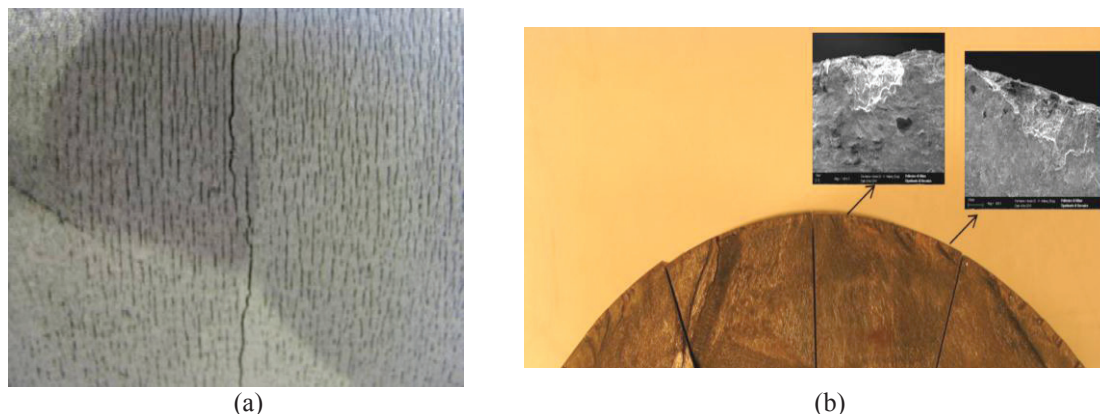


Fig.4. (a) Magnetic particles examination of the external surface of the specimen tested at constant amplitude of 160 MPa, after the final failure occurred at 9.4 million of cycles. (b) Crack surface and pits in the nucleation region.

The main fracture reveals a semielliptical crack (Figure 4(b)) with a depth of approx. 20 mm and with some other minor cracks near the ends. SEM observation of the ‘nucleation’ region reveals pits with a depth 50-100 μm . A section of the axles along its axis, reported in Figure 5, clearly shows a transgranular crack that in the first stage propagate inside an oxide path (interaction between corrosion and mechanical load) and in the second stage propagate more quickly than the oxide formation (mechanical effect is dominant). The variable amplitude test has been run with the load spectrum reported in Figure 6(a). The test has been interrupted at 14.6 10^6 , about 50% of the estimated life. At this stage, magnetic particles examination reveals numerous clusters of cracks having length of the order of millimeters, still not uniformly distributed.

4. Validation of the corrosion fatigue model

According to eq. (1) a prediction of the corrosion fatigue life of the full scale tests described in the previous paragraph can be also performed. For the constant amplitude full scale tests $\Delta\sigma=320$ MPa, the corrosion fatigue lifetime predicted by the model is of $6.3 \cdot 10^6$ cycles. The difference between the calculated and the experimental lifetime is less than the experimental scatter of data observed on small scale corrosion fatigue tests [4]. If the second experiment is considered, a prediction of the crack size vs. the number of cycles can be obtained according to the equation (1) and with the applied load spectrum reported in figure 6(a). In practice, the crack size is expressed in terms of depth a , with an appropriate correction assuming an aspect ratio of 0.85 as established in both in small and full scale experimental tests. The result is shown in figure 6(b). As previously said, in this case the estimated life is about $30 \cdot 10^6$ cycles and the test has been run for $14.7 \cdot 10^6$ cycles (half-life). At this stage the model predicts a corrosion fatigue crack length, on the surface of the specimen in the circumferential direction, of about 1.4 mm, while the experiment has shown the formation of a coalescence of small cracks crack about 1.5 mm long.

Conclusions

Two full scale corrosion fatigue tests of railway axles have been carried out. Crack growth rate measurements, enables us to set a modified version of a model proposed by Murtaza and Akid for the fatigue corrosion life prediction of railway axles. The corrosion–fatigue crack growth model enables us, also, to obtain a fairly precise prediction of the S–N diagram of A1T steel under corrosion–fatigue sustained by the free corrosion of the material.

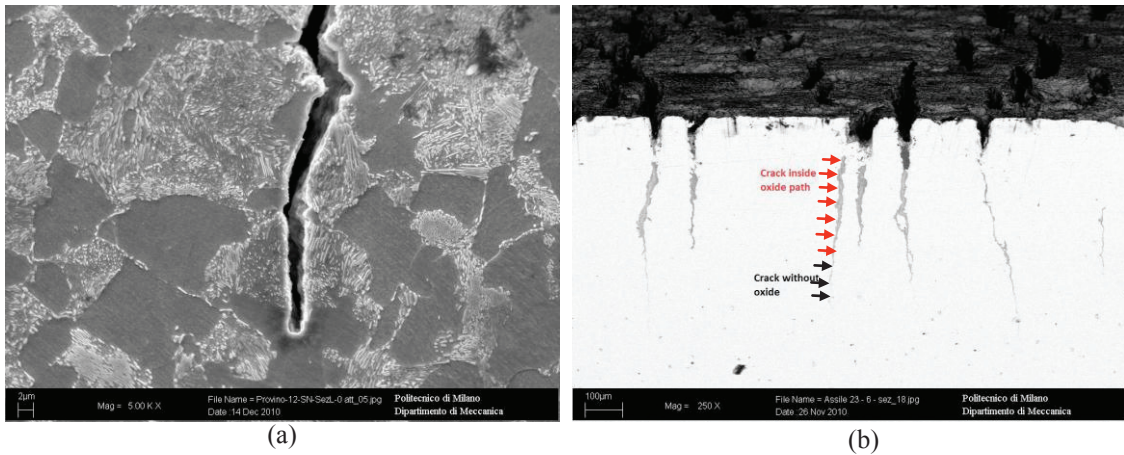


Fig.5. Section of the axles along its axis direction. (a) Transgranular path of the crack. (b) First stage of the crack growth inside a path of oxide and second stage more quickly of the oxide formation.

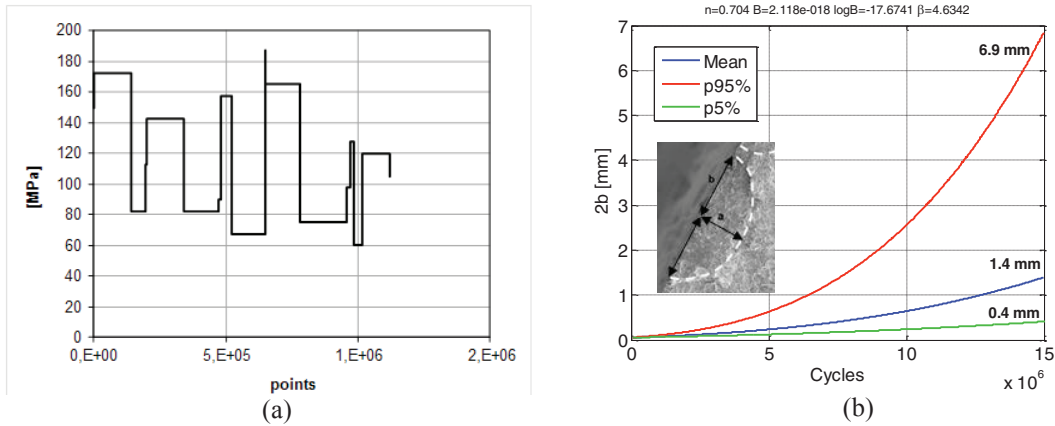


Fig. 6. (a) Load spectrum applied to the variable amplitude full scale test. ; (b) Crack growth rate, as predicted by the proposed model for the load spectrum of figure 8(a).

References

- [1] Hoddinot DS. Railway axle failure investigations and fatigue crack growth monitoring of an axle. *J Rail Rapid Transit* 2004;218:283–92.
- [2] Transportation Safety Board of Canada. Main track derailment: Canadian national train No. G-894-31-14. *Railway Investigation Report R01Q0010*; 2001.
- [3] Beretta S, Carboni M, Lo Conte A, Palermo E. An investigation of the effects of corrosion on the fatigue strength of A1N steel railway axles. *J Rail Rapid Transit* 2008;222:129–43.
- [4] Beretta S, Carboni M, Fiore G., Lo Conte A, Corrosion-fatigue of A1N railway axles steel exposed to rainwater, *International Journal of fatigue* 2010, 32.
- [5] Murtaza G, Akid R. Empirical corrosion fatigue life prediction models of a high strength steel. *Eng Fract Mech* 2000;67:461–74.